A versatile Lock-In digital Amplifier (LIdA)

The case of mechanical resonances

Bessas, D.; Brück, E.

DOI
10.1088/1361-6404/aa6606

Publication date
2017

Document Version
Accepted author manuscript

Published in
European Journal of Physics

A versatile Lock-In *d*igital Amplifier (LI*d*A): the case of mechanical resonances

D. Bessas*, E. Brück

February 20, 2017

Fundamental Aspects of Materials and Energy, Department of Radiation Science and Technology, Delft University of Technology, Mekelweg 15, 2629 JB Delft, The Netherlands.

Abstract

The assembly of a Lock-In *d*igital Amplifier (LI*d*A) from widely accessible ready-made modules is presented. This equipment, which does not require any advanced knowledge in electronics or programming, may introduce the experimenter to resonant techniques by registering mechanical resonances. The freely available control program allows for general data acquisition and further data processing. The apparatus is versatile and may corroborate the science and engineering laboratory in elasticity measurements or in a series of experiments where a modulated signal is a prerequisite.

1 Introduction

Resonances are of great importance both in fundamental and functional properties of a system and occasionally have a large impact on everyday life. A characteristic example in this respect is the destructive effect of mechanical resonances on large scale constructions such as bridges.

Resonant techniques are all along very well received by the scientific community and are relevant to electro-magnetic resonances, $e.g.$, electron paramagnetic resonance [1], nuclear magnetic resonance [2], with extensions up to high energy physics, $e.g.$, nuclear resonance scattering [3]. This is mainly because on a resonance, the signal to noise ratio maximizes and peculiar effects appear, which are otherwise inaccessible.

The concept of a resonance is indeed covered few times in the typical physics and engineering education, however, the importance of experimental resonant techniques are barely highlighted in the curriculum with possibly the only exception of resonances in electric circuits, $e.g.$, resistor - inductor - capacitor (RLC) circuits [4].

Despite the importance of experimental resonant techniques in research, a gap between the experimental scientific and engineering community and the undergraduate

*D.Bessas-1@tudelft.nl

education is generally observed. Such a gap may be reasonably attributed to the significant amount of effort and resources which needs to be invested in order to quantitatively register resonances. Arguably, the detection of resonances in research and development usually require sophisticated and expensive equipment or access to large scale facilities such as, high magnetic field laboratories, synchrotron radiation storage rings or high energy particle colliders. As a result the access to experimental resonant techniques is usually limited to a few people at later times in their careers.

Herein, we revive the case of mechanical resonances for a smooth transition of prospective scientists and engineers between the undergraduate curriculum and research. For this reason, the assembly of a low cost Lock-In $d$igital Amplifier (LIdA) from accessible ready-made modules is described. Such an equipment may not only serve educational purposes but it could also complement the scientific laboratory. Details on excitation and detection of mechanical resonances are given and the importance of mechanical resonances in research is further discussed.

2 Mechanical resonances and synchronous detection

A simple mechanical oscillator such as a mass, m, suspended by a spring which is driven by an external alternating force with amplitude F_0, and frequency f has a mechanical resonance at frequency $f_r = \sqrt{k/m}/2\pi$. It is already apparent that the knowledge of the resonant frequency provides a direct measure of the spring constant, k, which is both of fundamental and practical interest.

The frequency profile of the oscillating motion, $F(f)$, matches the Lorentzian profile $F(f) \sim F_0 f_r^2/(|f^2 - f_r^2| + f_r^2 Q^2)$, where $Q = f_r/\delta f_r$ is the resonance quality factor which is indicative of the full width at half maximum of the Lorentzian profile, δf_r. The well defined profile function of a resonance is an asset for resonant techniques. An additional asset is that on resonance, $i.e.$, at $f = f_r$, the amplitude of the resonating system is maximum. It is hence straightforward to assume that the detection of mechanical resonances might be an easy task. This assumption is indeed valid for qualitative observations, $i.e.$, when the amplitude of the excitation, F_0, is high enough and results in destructive phenomena, such as the case of falling bridges. However, in the case of non destructive techniques F_0 is kept low and consequently the quantitative detection of mechanical resonances is reduced in discriminating a small amplitude signal from the noise.

It is possible to distinguish a signal of small amplitude from noise both in time, as well as in frequency domain. Here, the analysis will be done in time domain since the transformation between time and frequency domain requires advanced mathematics [5], which might appear as a limitation for the unexperienced audience.

The main routes to distinguish a signal of small amplitude from noise in time domain is either the reduction of the noise amplitude or the so called synchronous detection. Although the reduction of the noise amplitude is always advisable, in most cases it is inherently difficult since some kind of noise, $e.g.$ thermal noise, electronic noise, $1/f$ noise [6] are practically unavoidable. The synchronous detection, which is also known as lock-in amplification, introduced by Cosens [7] and further simplified by Michels and Curtis [8] is thus the method of choice.

The working principles of a lock-in amplifier are extensively discussed in the literature and are beyond our scope herein. For a more detailed introduction into the principles of a lock-in amplifier the reader is encouraged to follow Ref. [9] and references therein. In short, a lock-in amplifier recovers a modulated signal with a well

defined modulation frequency and phase buried in a noisy carrier signal. The trigger and the recorded signals are multiplied. The resulting signal is filtered out for high frequency harmonics and all information relevant to the response of the studied system is encoded in the phase difference between the trigger and the recorded signal. The output of a lock-in amplifier comprises of a signal, I, in-phase to the reference signal, and a quadrature signal, Q, which is out-of-phase to the reference signal. The magnitude signal, R, is defined as $R = \sqrt{X^2 + Y^2}$, where X and Y are given as $R\cos\vartheta$ and $R\sin\vartheta$, respectively, and ϑ is the phase.

3 Excitation and detection of mechanical resonances

In order to excite and detect mechanical resonances from a solid one needs: a function generator, which produces modulated electrical signals of variable frequency, electromechanical transducers, which convert modulated electrical signals to analogous mechanical signals and vice versa, and a lock-in amplifier, which discriminates the actual signal from the noise.

Mechanical oscillations of solid bodies follow the classical wave mechanics equation, $u_s = l \cdot f_r$, with typical speed for the propagation of the wave front equal to the speed of sound, u_s. The resonant frequencies of solid bodies depend on the dimensions of the body itself, $i.e.$, the higher the dimensions, l, the lower the resonant frequencies. The volume of typical samples which are easy to obtain in the laboratory span between 1 mm^3 and a few cm^3. The typical speed of sound in solids ranges between 2 and 4 km/s. Thus, the typical resonant frequencies of such solids vary between 20 kHz and 2 MHz.

Commercially available lock-in amplifiers with high detection efficiency and accuracy exist [10], however, their wide use in the introductory laboratory is inhibited by their high cost. This is mainly due to the fact that the synchronous detection is realized through analog electronics, which except for price also adds in volume making such instruments non-portable. Lately, commercially available digital lock-in amplifiers appeared [11], however, the cost remained high. Several attempts for low cost both analog and digital lock-in amplifiers exist in literature, $e.g.$, Ref. [12, 13, 14, 15, 16, 17], however, most of them are dedicated to low frequencies, $i.e.$, well below 1 MHz. Such lock-in amplifiers may indeed be used for registering mechanical resonances in relatively large samples. However, large volume samples are not always available in the scientific and engineering laboratory.

4 Experimental setup

The overall experimental scheme for the excitation and detection of mechanical resonances is shown in Fig. 1a. A picture of the sample holder used for detection of mechanical resonances is depicted in Fig. 1b. A picture of the Lock-In $d$igital Amplifier (LIdA) assembly for registering mechanical resonances suggested in this study is shown in Fig. 1c.

The experimental setup comprises of a set of cylindrical S-type piezoelectric transducers [18] with a thickness of 0.4 mm and a diameter of 10 mm. The first mechanical resonance of such a transducer is 5 MHz, which is away from the mechanical resonances of the sample. The transducers were glued on plastic supports positioned on truncated cylindrical and hollow copper blocks. The lower copper block is a single

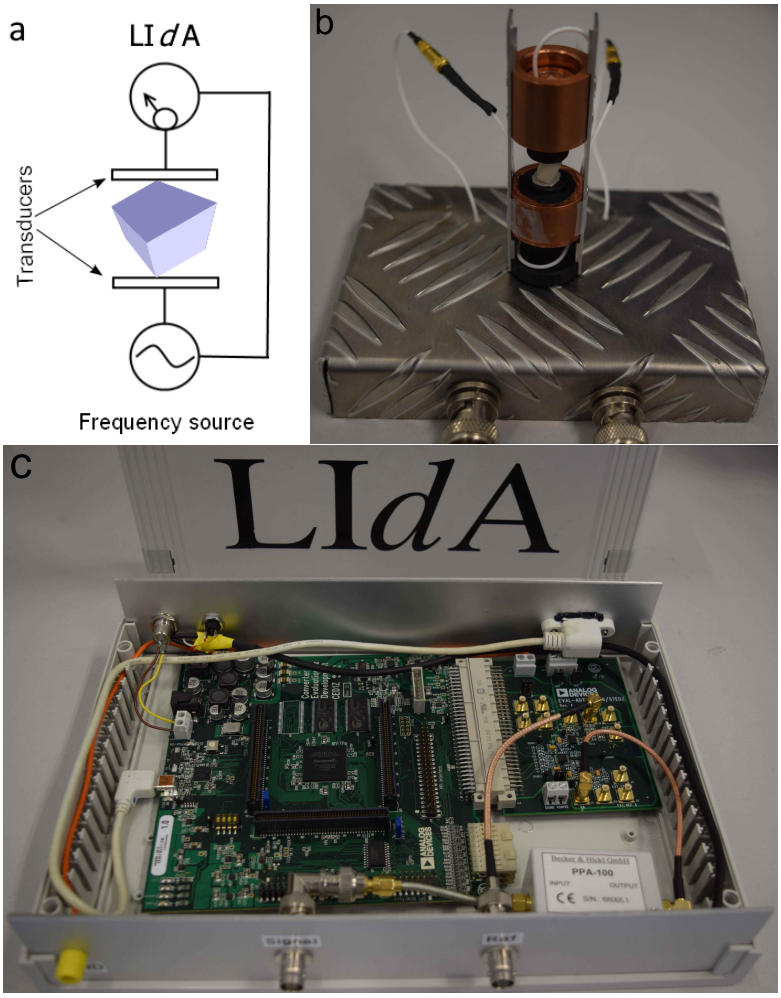

Figure 1: (a) The scheme of the spectrometer for exciting and recording mechanical resonances of solid samples includes a variable frequency source, a pair of piezoelectric transducers, and a Lock-In $d$igital Amplifier (LIdA). (b) A picture of the sample holder with the alumina sample mounted between the transducers. (c) The electronics assembly of LIdA.

piece, whereas the upper block is made of an inner and an outer part. The outer part is similar to the lower single part. Both parts are fixed using a primitive aluminum scaffold. The upper inner cylindrical piece is moveable. Such an elaborated design is not crucial for the operation of the spectrometer. It is only done in order to have the possibility to accommodate samples of various dimensions.

The excitation transducer, which is selected to be the lower one, is fed through a thin coaxial cable with a modulated electrical signal that is produced by a separate direct digital synthesis GF-266 function generator [19]. The coaxial cable may be either glued using a conductive glue or soldered at one side of the transducer. The other side of the transducer is grounded. The operation of both transducers is acoustically inspected by scanning the modulation frequency in the hearing range, $i.e.$, between 31 Hz and 21 kHz.

A reference signal with the same frequency and phase with the excitation signal is fed through a similar coaxial cable at one of the two channels, $i.e.$, Vb, of a commercially available ready-made 14-bit AD7357 digitizer [20]. The role of the digitizer is to convert the analog signal produced by the transducer to a digital one. For this specific digitizer the sampling frequency is 4.2 MHz. According to the Nyquist–Shannon sampling theorem [21] reliable data acquisition up to 2.1 MHz may be achieved with this specific digitizer.

The detection transducer, which is selected to be the upper one, is connected similarly as the lower transducer to a ready-made commercially available PPA-100 preamplifier [22]. The role of the preamplifier is to match the impedance difference between the piezoelectric transducer, which is in the range of several MOhm, to the input impedance of the digitizer, which is 50 Ohm, and to minimize potential electronic reflections due to impedance mismatch. The output of the preamplifier is connected using a coaxial cable to the other channel, $i.e.$, Va, of the digitizer. The digitizer is connected through a build-in 96 way connector to a commercially available Field-Programmable Gate Array (FPGA) CED1Z card [20] which has the same type of build-in connector. The acquired data are transferred through the FPGA card via a usb port using a usb cable to a personal computer for further processing and storage. Typical costs for all commercially available products in the assembly presented in this study is similar to the cost of a portable pc, $i.e.$, around €600[1]. The cost of cabling is negligible. The mechanical work for the sample holder was done manually on small spare parts and takes only a few hours. Notably, the overall volume of the electronics and the mechanical parts of the spectrometer presented in Fig. 1 including the preamplifier does not exceed the volume of a portable pc.

5 Control software

The experimental setup is controlled via a freely available [23] Labview-based executable which includes the tedious FPGA programming. In this respect the user may use the program as it is without any knowledge in programming or need for further development. The source code of the Labview executable [24] is also available in case the user would like to further customize it, $e.g.$, add a temperature or a magnetic field controller. The control panel of the Labview program is shown in Fig. 2. The graphical

[1] A set of piezoelectric transducers costs less than €5. The cost of a reliable function generator based on direct digital synthesis is in the range of €200. The cost of a digitizer card is in the range of €50. A commercially available preamplifier costs around €100. The cost of an FPGA card is in the range of €200.

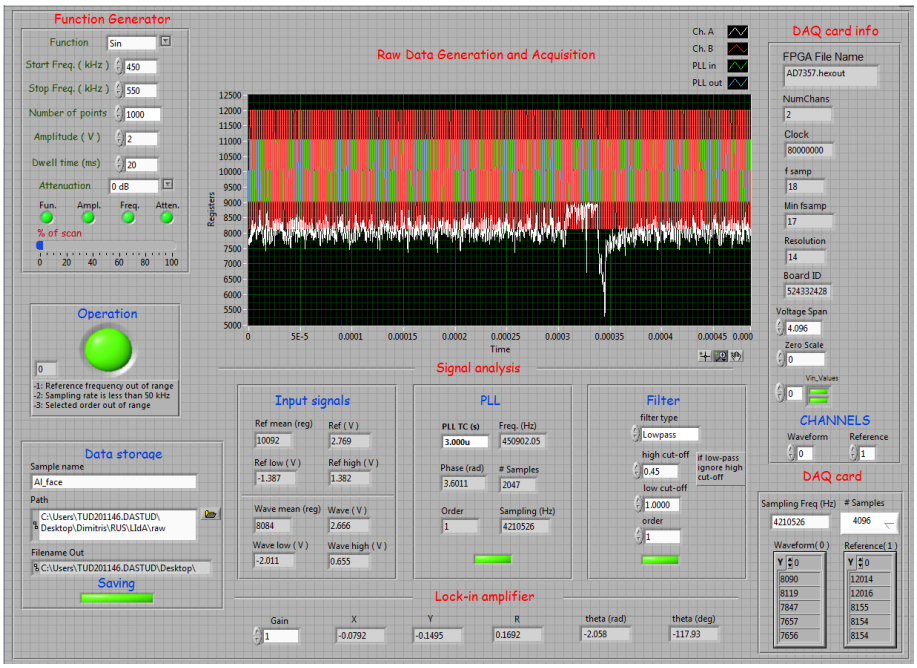

Figure 2: The graphical user interface of the freely available Labview program which controls the spectrometer. The white curve in the "Raw Data Generation and Acquisition" sub-panel corresponds to the response of the recording transducer whereas the red curve is the trigger signal. For more details on other sub-panels see text.

user interface is divided into sub-panels relevant to: the function generator, the data acquisition, the signal analysis, and the data storage. All white rectangular shaped areas are inputs and can be modified by the user whereas the grey areas are either outputs or contain information relevant to the experimental setup.

In the function generator sub-panel, the actual function can be selected, the initial/final frequency, the number of points, and the dwell time between the frequency points can be set. Moreover the amplitude or the attenuation of the output signal can be modified.

In the Data AcQuisition (DAQ) card info and the DAQ card sub-panel all information relevant to the digitizer and the FPGA card is given. The sampling frequency and the number of samples are set to their maximum values, 4.2 MHz and 4096 samples respectively.

In the signal analysis sub-panel the amplitude of the input signals, both for the reference signal and the recorded waveform, are shown. A Phase Locked Loop [25] (PLL) which detects the frequency and the phase of the reference signal is implemented. A variety of filter types, $e.g.$, low-pass [26], together with the order and the cut-off frequencies may be selected in the filter sub-panel and allows the user to filter out all the high frequency components in the lock-in process.

The program applies the synchronous detection in real time and the output of the lock-in process is provided in the lock-in amplifier sub-panel. Namely, the $X-$ and the $Y-$ components of the lock-in process, together with the magnitude signal, R, and the phase ϑ are given both in the control panel as well as in the output data file. More importantly, the raw waveforms shown in the data generation and acquisition sub-panel may be saved for future reference or further processing, $e.g.$, in the frequency domain.

6 Demonstration experiments and results

Solid samples exhibit mechanical resonances at resonant frequencies, f_r^i. The detection of the frequency profile on resonance depends crucially on the quality factor, $Q = f_r^i/\delta f_r^i$, which is in turn related to the micro-structure of the sample. Any solid sample of any shape may be used for demonstration experiments. Herein, a ceramic - polycrystalline - alumina (Al_2O_3), is selected on a trial and error basis. The demonstration sample is cut using a saw from a widely available large ceramic alumina piece. No further treatment, such as polishing, or any special care about the parallelism of the opposite sample faces is taken. The dimensions of the sample were measured with a caliper and found to be $4.40(5)$ mm $\times$ $5.56(5)$ mm $\times$ $7.74(5)$ mm. The mass of the sample was $0.654(5)$ g. The selected modulation function was of sinusoidal type with 5 V amplitude. A frequency scan was carried out between 300 kHz and 1.1 MHz with a 50 Hz frequency step. The overall spectrum was collected in less than 10 minutes.

The X- and Y- component and the magnitude signal R of the lock-in amplifier for the empty spectrometer with an open gap between the transducers is shown in Fig. 3a. The overall curves are rather smooth. The inset to Fig. 3a shows the frequency regions where small disturbances are observed. The disturbance regions are reproducible between different runs and can be most likely attributed either to small instabilities in the amplitude of the frequency source, the cross-talk of the excitation and detection transducer through the metallic scaffold, or less likely to environmental noise with the appropriate frequency and phase which successfully goes through the $lock-in$ amplifier. Fig. 3b shows the frequency response measured on the sample using the same sequence as in the background measurements. The sample was lightly held between its

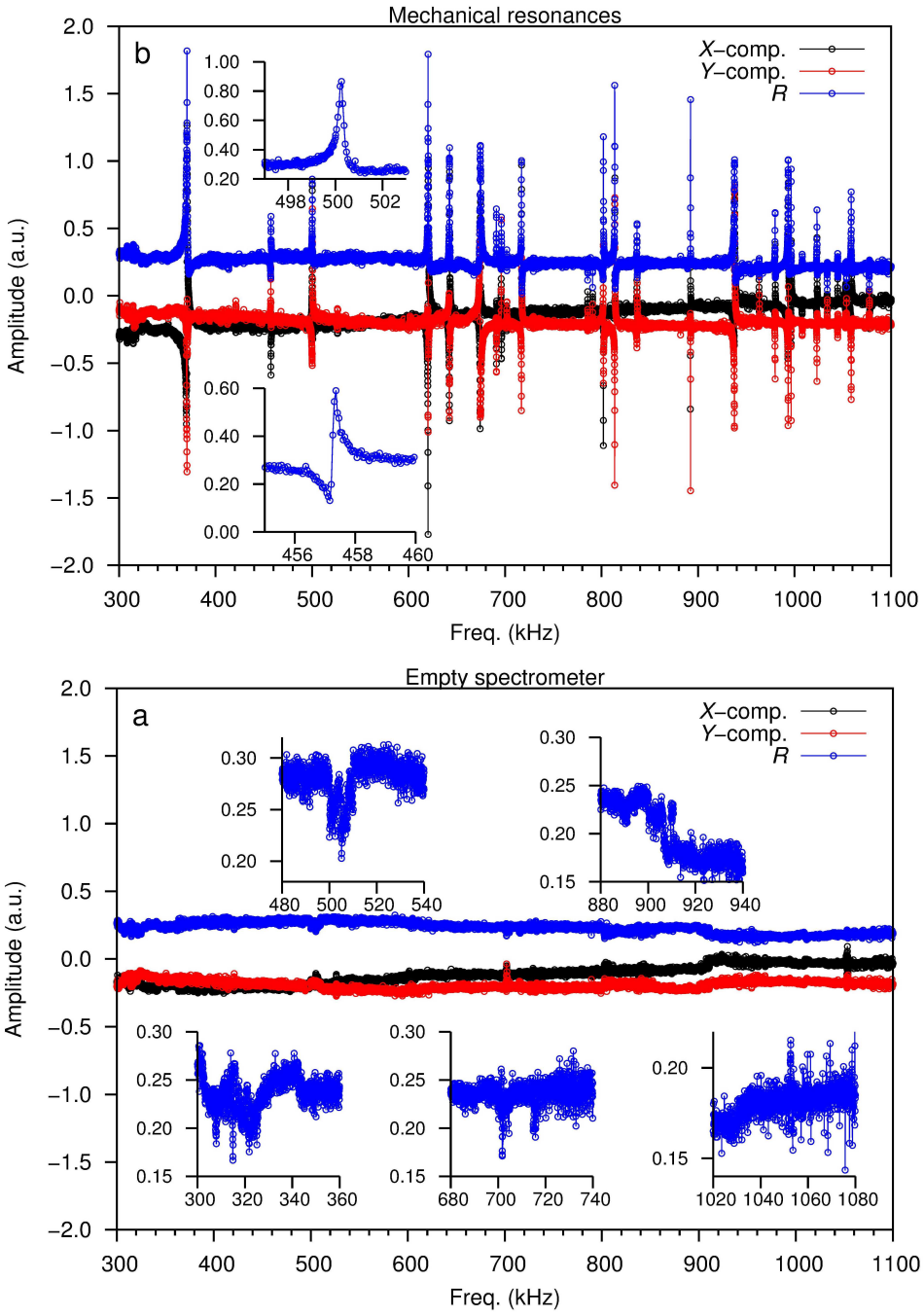

Figure 3: The X-, Y-, components and the magnitude signal R (see text) of the background spectrum measured on an empty spectrometer (a) and for the rectangular parallelepiped sample used in this study (b). Inset shows: (a) the maximum frequency disturbances caused by the setup (see text), (b) typical resonant lines. A line between the experimental points is given as a guide to the eye.

Table 1: The experimental resonant frequency, f_r^i, in MHz and the quality factor, $Q = f_r^i/\delta f_r^i$, for the first 14 mechanical resonances of a rectangular parallelepiped sample with dimensions $4.40(5)$ mm $\times$ $5.56(5)$ mm $\times$ $7.74(5)$ mm and mass $0.654(5)$ g.

i	f_r^i (MHz)	Q	i	f_r^i (MHz)	Q
1	0.370064	467	8	0.674416	2556
2	0.457166	2710	9	0.716967	5560
3	0.500151	2841	10	0.785485	6062
4	0.620242	5705	11	0.790638	21916
5	0.620372	30779	12	0.801774	5684
6	0.642341	7341	13	0.813615	4900
7	0.673962	1733	14	0.836681	5476

two opposite edges by the transducers. More than 25 sharp clearly resolved resonant lines can be identified between 300 kHz and 1.1 MHz. The first 14 resonances were fitted with a lorentzian profile using the portable command-line driven graphing utility Gnuplot [27] and both the resonant frequencies, f_r^i, and the quality factor, Q, are extracted and shown in Table 1.

7 Mechanical resonances and elasticity

Mechanical resonances are an indispensable tool in characterizing the elastic properties of a material. Mechanical oscillations follow classical mechanics. The equation of motion in this case is the Newton's law which in its differential form is given in Eq. 1.

$$\rho\omega_r^2\psi_i + \sum_{i,j,k} C_{ijkl}\frac{\partial^2\psi_k}{\partial x_j \partial x_l} = 0 \tag{1}$$

This is a typical eigenfunction, ψ, eigenvalue, ω_r, problem, which can be solved numerically and provides the frequencies of the mechanical resonances $f_r = \omega_r/2\pi$ if the elements of the elastic constants tensor, C_{ijkl}, and the mass density, ρ is known. The inverse problem may also be solved numerically. If the frequencies of the mechanical resonances, f_r, are measured on a sample of mass density ρ and a shape which can be described by a set of basis functions ψ then the elements of the elastic constant tensor C_{ijkl} can be extracted.

The elastic constant tensor in its general form has 36 elements. The number of independent elements, however, depends on the symmetry relation in the studied sample. For example, polycrystalline aggregates have only 2 independent elastic constants, namely, C_{11} and C_{44}, whereas the maximum number of independent elastic constants in the most anisotropic, triclinic, crystal structure is 21.

A program to refine the elastic constants of a rectangular parallelepiped solid is available online [28]. The output of the Los Alamos National Laboratory (LANL) Rectangular PaRallelepiped (RPR) code for refining the isotropic elastic constants (C_{11} and C_{44}) of the ceramic alumina sample measured in this study is shown in Fig. 4. The resonant frequencies shown in Table 1 together with the geometric dimensions and the sample mass are the input parameters to the program. The refined isotropic elastic constants at room temperature are $C_{11} = 467$ GPa and $C_{44} = 139$ GPa with an rms refinement error of 1.8%. The interested audience may find a more detailed manual on the use of this program in Ref. [29].

```
 LANL RPRcode Ver. 6.0
        ceramic
free moduli are  c11, c44
using 12 order polynomials     mass=  0.6540 gm  rho= 3.579 gm/cc

 n      fex       fr       %err  wt    k    i     df/d(moduli)
  1 0.370064 0.366815  -0.88 1.00  4    1   0.00   1.00
  2 0.457166 0.464584   1.62 1.00  1    2   0.15   0.85
  3 0.500151 0.507484   1.47 1.00  7    2   0.17   0.83
  4 0.620242 0.609119  -1.79 1.00  8    2   0.02   0.98
  5 0.620372 0.641019   3.33 1.00  5    1   0.08   0.92
  6 0.642341 0.653413   1.72 1.00  4    2   0.00   1.00
  7 0.673962 0.683416   1.40 1.00  2    2   0.03   0.97
  8 0.674416 0.686817   1.84 1.00  3    2   0.06   0.94
  9 0.716967 0.715468  -0.21 1.00  1    3   0.27   0.73
 10 0.785485 0.768063  -2.22 1.00  6    2   0.11   0.89
 11 0.790638 0.777087  -1.71 1.00  5    2   0.09   0.91
 12 0.801774 0.790671  -1.38 1.00  3    3   0.02   0.98
 13 0.813615 0.795739  -2.20 1.00  2    3   0.16   0.84
 14 0.836681 0.824657  -1.44 1.00  3    4   0.07   0.93

Bulk Modulus=    2.8152

   c11      c22      c33      c23      c13      c12      c44      c55      c66
4.67449 4.67449 4.67449 1.88550 1.88550 1.88550 1.39449 1.39449 1.39449

   d1       d2       d3
 0.44000  0.55600  0.74700

 loop# 4  rms error=  1.7904 %, changed by -.0000004 %

 length of gradient vector=  0.000000  blamb=  0.000000

 eigenvalues          eigenvectors
      0.00215   1.00 0.03
      3.00896  -0.03 1.00

chisquare increased 2% by the following % changes in independent parameters
  6.18 -0.56
  0.00  0.55
```

Figure 4: The LANL RPR code (Ver. 6) output from where the isotropic elastic constants of the ceramic sample are refined [28].

8 Discussion

The experimental setup described herein is assembled from commercially available pieces and programmed for synchronous detection. No need for advanced electronic design is required both for setting up and running the apparatus. It can thus be assembled and used both by undergraduate students and general physicists or unexperienced researchers. The control program is provided both as an executable for use as it is and as a source code for further research and development. The total cost of the equipment and its volume remains low. This fact makes the operation of multiple setups feasible and the setups portable. The experimenter will be familiar with terms such as instrument control, data acquisition, digital signal processing, and synchronous detection. The modular control program gives the opportunity for understanding the operation of various analog electronics, $e.g.$, frequency filters, without the actual presence of such analog devices.

The obtained data demonstrate the strength of resonant techniques. Although disturbances are recorded in an empty spectrometer, they do not follow a Lorentzian profile and thus are not of resonant nature. The sample oscillates at all frequencies, however, it is only at the resonant frequencies when the signal to noise ratio maximizes and a Lorentzian type frequency response is detected. In this respect the experimenter will be introduced in experimental resonant techniques and the concept of signal to noise ratio. The high precision and accuracy of resonant techniques may be further highlighted by illustrating the sensitivity of the resonant frequencies to changes in temperature and the change of the frequency response due to macroscopic defects such as chips and cracks.

Such a device apart from demonstration experiments may also be proven a useful tool for the advanced scientific research laboratory. Mechanical resonances are an indispensable tool for studying the elasticity of solids. A well established experimental technique known as resonant ultrasound spectroscopy [29], which focuses on the study of the coupling constants between stress and strain, $i.e.$, elastic constants, may be readily benefit from such a device. The elastic constants except from the obvious practical use in elasticity measurements are also of fundamental interest. Elastic constants complement the knowledge obtained by the lattice parameters, the inter-atomic position at which the global minimum in potential energy is observed, with the curvature of the potential energy at the global minimum.

In this configuration the setup is optimized for registering mechanical resonances of specimens with small volumes without requirements for advanced technical knowledge. The same electronic equipment, without hardware changes, may be used for general data acquisition. Once the electronic assembly is ready further measurements in a modulated mode, $i.e.$, resistivity/capacitance [30, 31], magnetic susceptibility [32], heat capacity [33], thermal diffusivity/conductivity [34] are accessible. Modulated signals of any type may be registered and a frequency analysis [5] may be carried out either in real time or at a later time.

9 Conclusions

The assembly, the control, and the operation of an open source Lock-In $d$igital Amplifier (LIdA) optimized for registering mechanical resonances is described. Such an apparatus may introduce the experimenter in resonant techniques and bridge the gap between education and research. The elastic constants of a system, which are both of

fundamental and practical interest, may be obtained using LIdA. Apart from mechanical spectroscopy LIdA may also be used in other areas of science and technology.

Acknowledgments

The technical assistance of Mr. J.-P. Celse and Mr. A. J. E. Lefering is acknowledged for the construction of the sample holder and the sample preparation, respectively. Mr. M. F. J. Boeije is acknowledged for a careful proofreading. The authors acknowledge financial support from the Industrial Partnership Program (IPP-I28) of Foundation for Fundamental Research on Matter (FOM) (The Netherlands) and BASF New Business.

References

[1] G. Lancaster, J. Mater. Sci. **2**, 489 (1967).

[2] H. Günther, *NMR Spectroscopy: Basic Principles, Concepts and Applications in Chemistry* (Wiley, 2013).

[3] R. Rüffer, C. R. Physique **9**, 595 (2008).

[4] P. Cafarelli, J.-P. Champeaux, M. Sence, and N. Roy, Am. J. Phys. **80**, 789 (2012).

[5] J. H. Scofield, Am. J. Phys. **62**, 129 (1994).

[6] M. van Exter, *Noise and Signal processing* (Universiteit Leiden, 2003).

[7] C. R. Cosens, Proc. Phys. Soc. **46**, 818 (1934).

[8] W. C. Michels and N. L. Curtis, Rev. Sci. Instrum. **12**, 444 (1941).

[9] S. DeVore, A. Gauthier, J. Levy, and C. Singh, Phys. Rev. Phys. Educ. Res. **12**, 020127 (2016).

[10] Http://www.thinksrs.com/products/SR844.htm.

[11] Http://www.thinksrs.com/products/SR865A.htm.

[12] G. Yang, J. F. Barry, E. S. Shuman, M. H. Steinecker, and D. DeMille, J. Instrum. **7**, 10026 (2012).

[13] K. Sowka, M. Weel, S. Cauchi, L. Cockins, and A. Kumarakrishnan, Can. J. Phys. **83**, 907 (2005).

[14] K. D. Schultz, Am. J. Phys. **84**, 557 (2016).

[15] M. J. Schauber, S. A. Newman, L. R. Goodman, I. S. Suzuki, and M. Suzuki, Am. J. Phys. **76**, 129 (2008).

[16] Y. Kraftmakher, Am. J. Phys. **74**, 207 (2006).

[17] B. K. Spears and N. B. Tufillaro, Am. J. Phys. **76**, 213 (2008).

[18] Https://www.steminc.com.

[19] Http://www.elc.fr.

[20] Http://www.analog.com.

[21] S. W. Smith, *The Scientist and Engineer's guide to Digital Signal Processing* (California Technical Publishing, 1997), ISBN 0-9660176-3-3.

[22] Http://www.becker-hickl.com.

[23] The executable is provided online.

[24] Http://www.bessasd.info/toolbox.html.

[25] S. M. Shahruz, Rev. Sci. Instrum. **72**, 1888 (2001).

[26] H. Krivine and A. Lesne, Am. J. Phys. **71**, 31 (2003).

[27] Http://www.gnuplot.info.

[28] Nationalmaglab.org/user-facilities/dc-field/dcfield-techniques/resonant-ultrasound-dc.

[29] A. Migliori and J. L. Sarrao, *Resonant Ultrasound Spectroscopy* (Wiley, 1997), ISBN 0-471-12360-9.

[30] J. Clayhold and J. Priest, Am. J. Phys. **76**, 1167 (2008).

[31] K. G. Libbrecht, E. D. Black, and C. M. Hirata, Am. J. Phys. **71**, 1208 (2003).

[32] M. Nikolo, Am. J. Phys. **63**, 57 (1995).

[33] Y. Kohama, C. Marcenat, T. Klein, and M. Jaime, Rev. Sci. Instrum. **81**, 104902 (2010).

[34] U. Zammit, M. Marinelli, R. Pizzoferrato, F. Scudieri, and S. Martellucci, Phys. Rev. A **41**, 1153 (1990).